# Application of the Vectorial J-integral to Adhesive Bonds

Z. W. CHEN* and R. D. ADAMS**
*BAMEDC P.O. Box 9226, Beijing, 100076, PRC
**Department of Mechanical Engineering, University of Bristol
BS8 1TR, UK

ABSTRACT

A fracture mechanics approach using the vectorial J-integral has been discussed in detail, particularly in connection with complicated singular problems in adhesive bonds. Some numerical results presented agree well with existing methods when these are available. A procedure parallel to conventional LEFM has been established to apply the present approach to engineering applications.

KEYWORDS

Fracture, J-integral, adhesive, numerical analysis, singularity

## INTRODUCTION

In elastic-plastic fracture mechanics(EPFM), the stress distribution around a crack tip is then given by the HRR solution(Rice and Rosengren,1968; Hutchinson 1968):

$$\sigma_{ij}(r,\theta) = \sigma_o \left(\frac{J}{I_n r \sigma_o}\right)^{\frac{n}{n+1}} \cdot g_{ij}(\theta) \qquad (1)$$

where $I_n$ is a function of n, n is the strain hardening exponent, $\sigma_o$ is a constant,
$g(\theta)$ are functions of direction only, and
J is a path independent integral.

The equation demonstrates a singularity in r which is often called the HRR singularity such that J is the strength of this singularity. The J-integral can also be viewed as the energy

available to make the crack propagate. Accordingly, the failure criterion becomes

$$J \geq J_c \qquad (2)$$

where the critical value $J_c$ is a material property and is called the fracture toughness.

Eshelby(1956) discussed general defects in an elastic continuum, including dislocations and inhomogeneities. The energy momentum tensor of an elastic field is derived as

$$J_i = \int_S (Wn_i - n_k \sigma_{jk} \frac{\partial u_j}{\partial x_i}) \, dS \qquad (3)$$

where u is the displacement vector
n is the directional cosine of the outward normal of the boundary surface S, and
W is the energy density.

The J vector gives the force on all sources of singularities and inhomogeneities within the enclosed surface S arising from an external stress system. In particular, the J vector is not necessarily only associated with cracks but it is the measure of all sources of any kind of singularity which may be caused by anydiscontinuity enclosed by the surface S. Rice's J-integral is a special case in 2-dimension with the crack tip as the only singular source such that $J_2$ and $J_3$ vanish and surface integration degenerates into a line integration.

In adhesive bonds, there is always a discontinuity in material properties regardless of whether there is a crack or not. Hereafter, the 'singularity' will be used to mean any discontinuity which cannot be accounted for by continuum mechanics and the J vector will be used to investigate this singularity.

The failure criterion for a homogeneous material using the J vector method can be expressed as

$$|J| \geq J_c \qquad (4)$$

where $|J|$ denotes the modulus (magnitude) of the J vector.

## NUMERICAL PROGRAM AND ANALYSIS

A 2-dimensional finite element program FELDEP is available for the stress analysis of adhesively-bonded joints. A FORTRAN program JINTEG has been developed for use in association with FELDEP to calculate the J vector. In order to check the correctness of the program, a systemmatical analysis on a standard fracture specimen was performed.

The fracture testpiece is a single edge notched three point



bending fracture toughness test specimen (SENB). The systemmatical analyses include four cases using small displacement elasticity theory (se for short), large displacement elasticity theory (le for short), small displacement plasticity theory (sp for short), and large displacement plasticity theory (lp for short).

The specimen was made from a rubber modified epoxy adhesive (designated as CTBN here) for which E = 2500 MPa and $\nu$ = 0.37. The stress-strain curve used for the plastic analysis is obtained experimentally. In the finite element model, only half of the SENB specimen has been modelled and the x-axis was taken within the symmetry plane. The specimen was loaded under plane strain condition to the fracture load determined expermentally which corresponds to a load of 36 N per mm thickness. This load gives K=2.215 $MN/m^{3/2}$ according to well-known expression(ASTM). This is equivalent to J = 1.672 $(kJ/m^2)$.

As all the paths specified were half of the closed paths, all the numerical values of $J_i$ from JINTEG should be multiplied by a factor of two. 10 paths were used to calculate and average $J_i$ for all 4 cases. The output from JINTEG is in Table 1.

Table 1. Numerical J Values for SENB Specimen

| | | $J_1$ | | | | $J_2$ | | | |
|---|---|---|---|---|---|---|---|---|---|
| | length | se | le | sp | lp | se | le | sp | lp |
| 1 | 3.027 | 0.836 | 0.820 | 0.842 | 0.827 | 0.025 | 0.039 | 0.025 | 0.039 |
| 2 | 2.049 | 0.833 | 0.815 | 0.839 | 0.822 | 0.019 | 0.036 | 0.019 | 0.035 |
| 3 | 8.303 | 0.833 | 0.823 | 0.840 | 0.830 | 0.037 | 0.047 | 0.037 | 0.047 |
| 4 | 4.638 | 0.823 | 0.811 | 0.830 | 0.818 | 0.030 | 0.041 | 0.029 | 0.041 |
| 5 | 16.852 | 0.831 | 0.824 | 0.837 | 0.830 | 0.049 | 0.058 | 0.049 | 0.059 |
| 6 | 11.590 | 0.828 | 0.820 | 0.835 | 0.827 | 0.042 | 0.051 | 0.042 | 0.052 |
| 7 | 31.496 | 0.830 | 0.827 | 0.837 | 0.834 | 0.062 | 0.071 | 0.063 | 0.073 |
| 8 | 22.186 | 0.828 | 0.823 | 0.835 | 0.829 | 0.055 | 0.064 | 0.055 | 0.065 |
| 9 | 33.971 | 0.831 | 0.829 | 0.838 | 0.842 | 0.057 | 0.065 | 0.058 | 0.066 |
| 10 | 33.196 | 0.830 | 0.827 | 0.836 | 0.840 | 0.066 | 0.076 | 0.067 | 0.075 |
| Average | | 0.830 | 0.822 | 0.837 | 0.830 | 0.044 | 0.055 | 0.044 | 0.055 |

Units: mm for length and $KJ/m^2$ for J-integral

It can be noticed: a) With path lengths ranging from 2.05 mm to 33.97 mm, path independence was proved for all 4 analyses as the maximum deviation was only about 1.0%. b) For the specimen and material concerned, the non-linear analyses made little difference. The SP analysis results gave a minor improvement of 1% over the SE analysis, judging from the average of 10 paths. c) Comparing the numerical results with ASTM expression as given in Table 2 shows good agreement. The difference between ASTM result and the averaged J vector for the case sp is less than 0.5%.

All the above points show that the program is reliable and the numerical results are accurate.

Table 2. Comparison of J and $\theta$

| cases | $J_1$ KJ/m$^2$ | $J_2$ KJ/m$^2$ | $\|J\|$ KJ/m$^2$ | angle $\theta$ degree |
|---|---|---|---|---|
| s.e. | 1.6606 | 0.0882 | 1.6630 | 3.04 |
| l.e. | 1.644 | 0.1098 | 1.6474 | 3.82 |
| s.p. | 1.674 | 0.0889 | 1.676 | 3.04 |
| l.p. | 1.660 | 0.1103 | 1.6636 | 3.80 |
| ASTM | 1.672 | 0.0 | 1.672 | 0.0 |

The direction of the J vector can be determined. The angle $\theta$ predicts the direction of crack propagation. Within a maximum deviation of 4° as shown in Table 2, it agreed fairly well with the theoretical 0 degree. This demonstrates that the J vector criterion itself can be considered as a mixed-mode failure criterion. Most adhesive bonding problems inherently involve mixed-mode fracture and most of them are not separable into different modes in order to apply other mixed-mode fracture criteria.

## BONDED SYSTEM

Considering a bi-material system without cracks, the energy conservation law can be applied to individual homogeneous materials and this gives

$$\int_S \left(Wn_i - n_k\sigma_{jk}\frac{\partial u_j}{\partial X_i}\right) dS + \int_{S_o}\left([W]^+_-\cdot n_i - [\sigma_{jk}n_k\frac{\partial u_j}{\partial X_i}]^+_-\right)dS=0 \qquad (5)$$

where $[\ ]^+_-$ denotes the jump of a function across the bonding interface $s_o$. Without any other singularity in the system, equation (5) reveals that

$$J_i = -\int_{S_o}\left([W]^+_-\cdot n_i - [\sigma_{jk}n_k\frac{\partial u_j}{\partial x_i}]^+_-\right)ds \qquad (6)$$

If the two materials have the same properties, the jump across the interface will be zero so that the $J_i = 0$. For different materials bonded together, the J vector is not zero. This can only be expected because the interface is a kind of singular source. This singularity will be discussed in detail in terms of the numerical $J_i$ results.

A specimen modelled as half CTBN and half steel bonded together was loaded by applying a uniformly distributed tension (T) along the CTBN boundary as shown in Fig.1. The left hand boundary of the steel was restrained in the x-direction. The CTBN had the same propertied as before, and the steel properties were: E = 210 GPa; $\nu$=0.33 .

### Elastic Analyses

Linear elastic analyses were carried out for the bonded specimen . The stress distribution diagrams shown in Fig.2 are for an applied stress, T, of 15 MPa. The obvious singularity at point A is clrarly seen. The singlar nature of the bond line



will become clear when the $J_i$ numerical results are examined.

The values of J in Table 3 are for an applied stress, T, of 30 MPa. As the bond line was parallel to the y-axis, the path independence of $J_2$ indicated that all the singularity in the y-direction was at the point A. It can also be seen that the values of $J_1$ vary with the path length. A close look at Table 3 will reveal that although the paths 7, 9, and 10 had different lengths, while enclosing the same bond line, the values of $J_1$ for these three paths were practically the same. This means that $J_1$ is also path independent as long as the same bond line is enclosed by the different paths, $J_i$ is dependent on bond line length only.

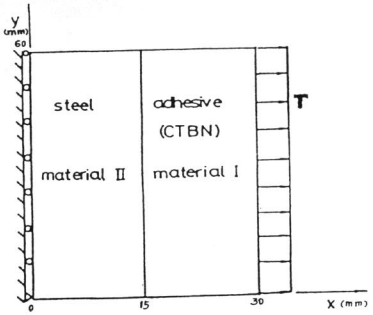


FIG.1 SIMPLE TWO-MATERIAL BOND

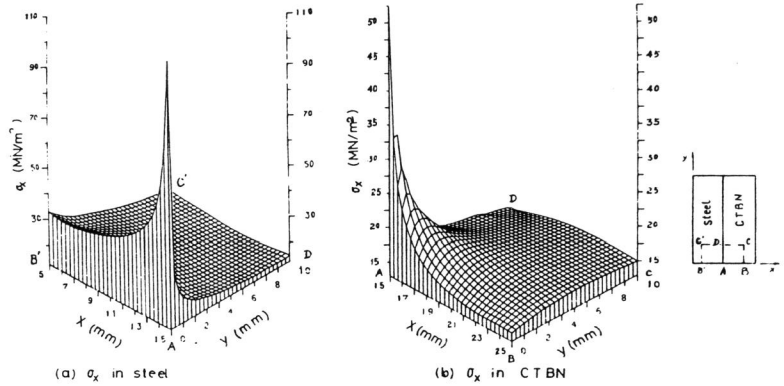


Fig.2 Elastic stress distribution in the simple bond

Another point is the direction of the J vector. $J_i$ was extrapolated against interface length to get $J_i$ for the point A. The direction of the J vector is given by $\theta=\tan^{-1}(J_2/J_1)$ which is 126.5° for point A. If the steel had the same fracture toughness as CTBN, the predicted crack would initiate and propagate in the steel ($\theta$>90°). This is consistent with the common knowledge that the failure would be in the stiffer material if the

Table 3. Numerical J values for Bonded System

| NO. | path length mm | bond line mm | $J_1$ KJ/m$^2$ | $J_2$ KJ/m$^2$ |
|---|---|---|---|---|
| 1 | 4.848 | 0.965 | -1.070 | 0.400 |
| 2 | 3.270 | 0.653 | -0.924 | 0.397 |
| 3 | 11.949 | 2.848 | -1.609 | 0.401 |
| 4 | 7.110 | 1.553 | -1.265 | 0.394 |
| 5 | 23.16 | 5.781 | -2.126 | 0.401 |
| 6 | 16.263 | 3.981 | -1.827 | 0.398 |
| 7 | 42.316 | 10.765 | -2.750 | 0.401 |
| 8 | 30.137 | 7.598 | -2.372 | 0.398 |
| 9 | 48.492 | 10.765 | -2.760 | 0.409 |
| 10 | 45.411 | 10.765 | -2.762 | 0.410 |

two blocks had the same toughness.

In practice, the fracture toughness of the materials will not be the same, so the failure will not propagate in the same direction as the J vector since it depends also on the fracture resistance of the materials. Then we can define the fracture toughness as a function of direction and position for a complex material system, such that

$$J_c = J_c(\theta, x, y, z) \tag{7}$$

In the bi-material system considered here, for instance at point A, it is simplified to

$$J = \begin{cases} J_c \text{ of CTBN} & \text{if } 0^\circ < \theta < 90^\circ \\ J_c \text{ of steel} & \text{if } 90^\circ < \theta < 180^\circ \end{cases}$$

At $\theta=90^\circ$, the fracture toughness depends on many factors such as the physical and chemical characteristics of the bonding interface, surface preparation, and defects in the bonding. For a perfect bond, it can be assumed that $J_c = J_c$ of CTBN.

To be able to use the J vector as a fracture criterion, we must convert the J vector into a direction related scalar. This can be done by projecting J onto a straight line in the direction of $\theta$ (whose direction cosine is denoted as $n_i$), such that

$$J(\theta) = J_i n_i \tag{8}$$

$J(\theta)$ can then be considered as the singularity driving force in the direction $\theta$. In the present two-dimendional case, equation (8) becomes

$$J(\theta) = J_1 \cos\theta + J_2 \sin\theta \tag{9}$$

It is worth mentioning that Kishimoto (1980)has obtained the sameform of equation based entirely on different arguments.

The fracture criterion is now generalized as

$$J(\theta) \geq J_c(\theta) \tag{10}$$

and the failure will occur in the direction in which condition (10) is first reached. It must be emphasized that both J and



$J_c$ are local parameters, in other words they are functions of position for nonhomogeneous materials. When there are different singular sources operating together, such as crack, voids and the bonding interface, the theory takes the same form to account for them all. This advantage makes the present approach superior to some other approaches for a complicated system,for example, to predict the failure of a composite material. In macromechanics, a composite is considered as homogeneous but highly anisotropic. The macro fracture toughness $J_c$ is not a function of position but is a function of direction. Most composites fail in an interlaminar fashion since this is the direction in which $J_c$ is the least. On a micro scale, a composite has many kinds of singularities, such as microcracks, voids, interfaces, debonding and so on. Conventional fracture mechanics is no longer sufficient to deal with all of these.However, there is no difficulty in applying the present method.

In LEFM, the relationship of J and the applied stress T can be expressed as

$$J \propto T^2 \text{ or } J = T^2 Y/E' \tag{11}$$

where $E' = E$ for plane stress, or $E/1-\nu^2$ for plane strain, and Y is a function to account for the nature of the singularity and the geometric configuration.

In the LEFM regime, Y is a constant for a particular geometry and material combination, so it can be derived by carrying out a numerical J integral for an arbitrary applied load. For example, for the bi-material bond here, $Y_1$ and $Y_2$ were derived from an applied load of 30 MN/m$^2$.

Once the value of Y is known for a given system, J is directly related to the applied stress by equation (11), so it is easy to estimate J for different applied loads. A comparison of values of J between those estimated using equation (11) and those obtained from the actual numerical integration is in Table 4.

Table 4. Numerical and predicted J

| Load | $J_1$Numerical | $J_1$(eq.11) | $J_2$Numerical | $J_2$(eq.11) |
|---|---|---|---|---|
| MN/m$^2$ | KJ/m$^2$ | KJ/m$^2$ | KJ/m$^2$ | KJ/m$^2$ |
| 15 | -0.267609 | -0.2676 | 0.100 | 0.100 |
| 30 | -1.07044 | -1.07044 | 0.401 | 0.401 |
| 39 | -1.80904 | -1.809 | 0.6776 | 0.6777 |
| 48 | -2.74032 | -2.740 | 1.0264 | 1.0266 |

From Table 4 it can be seen that equation(11) gives excellent results. Therefore, a simple method for dealing with the singularity in adhesive bonds which can be used in engineering design and analysis has also be established. This approach is similar to conventional LEFM but different in that there is no crack length (in fact, no crack at all). This has not been done before to the authors knowledge.

## Plastic Analyses

The geometry considered here is the same as for the elastic cases, and the steel is treated as being linearly elastic. The elasto-plastic stress-strain curve for CTBN is the same as before. As the plastic zone is bigger for this configuration than for the SEBN specimen (because of the weaker singularity without a crack), the plastic effects can be clearly seen now. The contour plot of plastic energy density in Fig.3 is under an applied nominal stress T of 48 MPa and shows how big the plastic zone is.

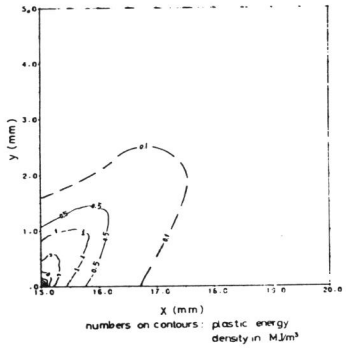


Fig.3 Contour plot of plastic energy density in CTBN showing the plastic zone.

$J_i$ values for all 10 paths at an applied stress, T, of 48 MPa are shown in Table 5. The integral paths 1, 2 and 4 had passed through the plastic zone. Table 5 shows that the path independence of $J_2$ is retained even for those paths through the yield zone. The numerical values of $J_i$ for path 10 for various applied loads are compared with the elastic results in Table 6 . Since J is dependent on the bond line length, this comparison can only be made for a specified path (path 10 here). Table 6 shows that in plastic analyses, values of J were greater than for the elastic analysis, especially for $J_2$ which acts to separate the two materials along the bond line interface.

Table 5. Numerical J for plastic analysis

| No. | path length mm | interface mm | $J_1$ KJ/m$^2$ | $J_2$ KJ/m$^2$ |
|---|---|---|---|---|
| 1 | 4.848 | 0.965 | -2.472 | 1.826 |
| 2 | 3.270 | 0.653 | -2.096 | 1.797 |
| 3 | 11.949 | 2.848 | -4.002 | 1.855 |
| 4 | 7.110 | 1.553 | -3.031 | 1.823 |
| 5 | 23.155 | 5.781 | -5.447 | 1.874 |
| 6 | 16.263 | 3.981 | -4.623 | 1.659 |
| 7 | 42.316 | 10.765 | -7.150 | 1.884 |
| 8 | 30.137 | 7.598 | -6.275 | 1.872 |
| 9 | 48.492 | 10.765 | -7.172 | 1.911 |
| 10 | 45.411 | 10.765 | -7.177 | 1.914 |

Table 6. Comparison of J values for the path No.10

| Load MN/m | $J_1$ Elastic KJ/m$^2$ | $J_1$ Plastic KJ/m$^2$ | $J_2$ Elastic KJ/m$^2$ | $J_2$ Plastic KJ/m$^2$ |
|---|---|---|---|---|
| 15 | -0.6905 | -0.6905 | 0.1024 | 0.1054 |
| 30 | -2.7618 | -2.7659 | 0.4097 | 0.5434 |
| 39 | -4.6675 | -4.6902 | 0.6924 | 1.0966 |
| 48 | -7.0703 | -7.1768 | 1.0488 | 1.9138 |



In Fig.4, $J_2$ is plotted as a function af $T^2$. It can be seen that the EPFM results differed signicantly from the LEFM results when excessive yielding takes place. Plastic effects must therefore be taken into account and the LEFM methods are no longer applicable. From Fig. 4, the function $Y_2$ can be determined for the geometry and material combination concerned. In Fig.5, $Y_2$ is no longer a constant but varies with applied load because of the material plasticity. For a non-linear system, a series of analyses is needed in order to obtain the Y function.

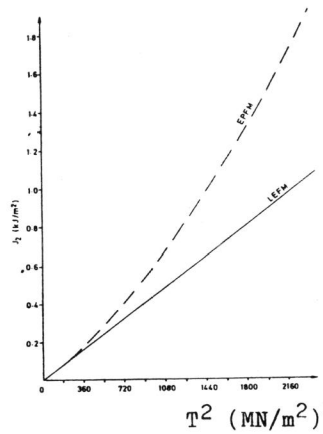


Fig.4 Comparison of elastic and plastic $J_2$ values

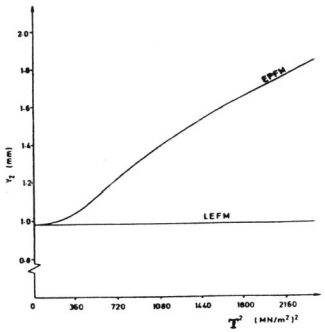


Fig.5 $Y_2$ function against $T^2$ for the simple bond.

Numerical methods can be used to derive 'the shape function' Y curve for any particular combination of materials and geometry. Once the $Y_i$ functions have been determined, they can be used to estimate $J_i$ in engineering applications using eq.(11) as in elastic cases. The present approach is promising in dealing with complex singular problems.

## REFERENCES

ASTM Standard E399-74 (1974), Annual Book of ASTM Standards, Part 10

Eshelby, J.D. (1956) in: Solid State Physics Vol.3 pp.79-144 Academic Press, New York

Hutchinson, J.W. (1968) J. of Mechanics and Physics of Solids , 16 pp 13-31

Kishimoto, K. et al (1980), Engg.Frac. Mech.13 pp841-850

Rice, J.R. and Rosengren, G.F.(1968), J. of Mechanics and Physics of Solids 16 PP.1-12